AIAA 82-4013

Electromagnetic Interference Signal Frequencies Caused by Discharges within Spacecraft

M.J. Schmidt* and H.W. Bloomberg†
Science Applications, Inc., McLean, Va.

The electron caused electromagnetic pulse (ECEMP) internal response of a cluttered cavity with the geometry characteristics of a spacecraft (DSCS II) is computed and analyzed for a typical current distribution caused by dielectric discharge. A pulsed discharge across a narrow gap in the cavity interior is considered, and the frequency of the response is found to be much lower than expected from the lowest mode of an uncluttered cavity. The effect can be thought of as due to the "loading" of a basic coaxial cavity by the impedances corresponding to the cluttering structures. The phenomenon is considered analytically and numerically for the simple case of capacitive loading due only to a narrow gap. It is shown that for special cases, the problem of frequency response can be reduced to the matching of the impedance characterizing the coaxial cylinder with the impedance of the narrow gap.

I. Introduction

IT is well known that differential charging can lead to large potential differences between adjacent sections in spacecraft at synchronous altitudes.[1] For a large enough potential buildup, a current discharge can occur.[2,3] Besides causing local damage, the discharge can be a source of electromagnetic radiation throughout the inside of the spacecraft. The resulting electromagnetic interference (EMI) is an acknowledged problem in spacecraft design. The electric field component of this radiation can have deleterious effects upon the electronic system. In addition, the magnetic field component can give rise to surface currents of sufficient strength to be harmful to the internal circuitry.

Unfortunately, until now there has been little data on the electromagnetic response of satellite systems due solely to the internal discharge component of the source. Simulation experiments that produce breakdown often give rise to strong external blowoff effects as well.[4] It is not clear to what extent this phenomenon can couple back into the cavity and mask the discharge effect. On the other hand, Stevens[5] recently has indicated that external blowoff in actual satellites can be substantially reduced from those values in worst case simulation tests. This implies that the effect of internal discharge, while also reduced, may be the dominant contribution to the electromagnetic interference.

Numerical techniques to handle the EMI problem have been developed even for the complicated cluttered geometries characteristic of spacecraft. Still, few results have been reported in the literature, because of the difficulty in giving a general, nontrivial interpretation to a problem that contains a multitude of parameters, including those associated with cluttered geometries and the specification of the discharge mechanism. In this paper, we show that an EM response to dielectric discharges can be significantly altered in cavities with internal cluttering. In particular, we find for a typical configuration that the characteristic eigenmode frequency within a cluttered geometry can be much lower than the frequency corresponding to the lowest mode of the cavity when empty. We offer an explanation for this effect in terms of a circuit analogy which is general enough to give useful EM response information for a large class of discharge problems in cluttered geometries.

Here, we examine the properties of the electromagnetic field generated within a spacecraft due to a typical discharge pattern. In Sec. II, we model the spacecraft interior by a perfectly conducting cylinder within which the two-dimensional cluttered structure characteristic of the DSCS II is included (see Fig. 1). The discharge is assumed to occur across a narrow-gap, high-capacitive element positioned near one of the cylindrical faces. This configuration corresponds to the DSCS II onboard thermal blanket, where discharges have been found to occur in experiments.[6] The electromagnetic code[7] used in the calculation is well suited to the spacecraft EMI problem because changes in the cluttered geometry can be implemented rapidly in the input section of the algorithm. At every time interval, field information is printed out at selected points. In addition, field contours are plotted within the space of the cluttered geometry, which are exhibited explicitly. The results of the calculation stressing the reduction in the expected frequency response are also presented in this section.

In order to explain the results qualitatively, a simplified cavity model consisting of coaxial cylinders with a small gap at one end is introduced in Sec. III. An analytic expression for the impedance of the coaxial system is defined near the surface of the inner core. We explain how the frequency response is obtained by computing the impedance associated

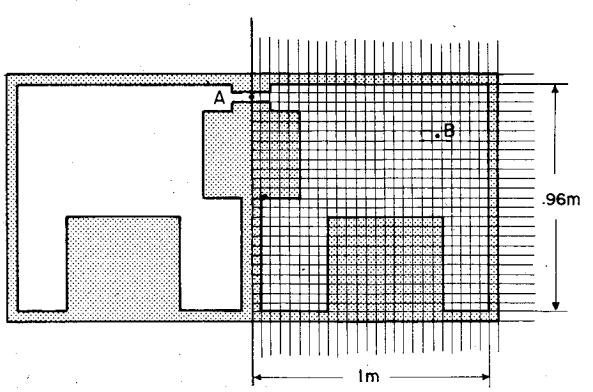

Fig. 1 Cylindrically symmetric cavity used for spacecraft charging problem. Discharge occurs at position A. Mesh superimposed on right of cavity is the computer grid used to difference the electromagnetic fields. Position B is an observer location for magnetic field.

Received Jan. 15, 1981; revision received June 18, 1981.

*Research Scientist, EM/Radiation Effects Division.
†Research Scientist, Mission Research Corp., Alexandria, Va.

with the gap and then invoking the principle of impedance matching. The main conclusions of this work are noted in Sec. IV.

II. Numerical Model and Results

In order to simulate the spacecraft charging problem, we approximate the interior of the satellite by the cylindrically symmetric configuration shown in Fig. 1. The shaded area represents the spacecraft's metallic structure. The discharge takes place in the region marked A in this figure. As the discharge occurs, it radiates electromagnetic energy into the interior of the satellite. We compute the radiation from such a current source using an electromagnetic code[7] that solves Maxwell's equations in cylindrical coordinates.

The spatial differencing grid used by the code is shown on the right of Fig. 1. The dimensions of one cell are 4×4 cm. There are 26 grid divisions in both the r and z directions. A combination of azimuthal symmetry and axial driving current will excite only the E_r, E_z, H_θ field triad which represent Transverse Magnetic (TM) modes. The H_θ field is defined on the center of each cell. The E_r field is defined on radial edges of each cell. The E_z field is defined on the axial edges of each cell.

The method the code uses to introduce structures into the interior of a cylindrical cavity is to clamp the E field to zero on the edges of those cells that are specified as metallic by the input data. This is the correct boundary condition for conducting surfaces since only tangentical E fields are defined on the cell edges. Referring to Fig. 1, all of the grid cells in the shaded areas were defined as metallic by the input data for the problem. Any change in the internal geometry can readily be implemented by a change in this input data.

The discharge current is represented at point A in Fig. 1 by an axial current density J_z whose pulse shape is

$$J_z(t) = 61.5\times10^4 \mid \exp(-10^6 t) - \exp(-2.66\times10^8 t) \mid \quad (1)$$

This current pulse has a rise time of 3.75 ns, a pulse width of 520 ns, and a maximum amplitude of 60×10^4 A/m^2. Equation (1) is graphically displayed in Fig. 2. This representation is thought to be characteristic of the internal discharges in simulation experiments at the Air Force Weapons Laboratory with an amplitude corresponding to a worst case configuration.[8]

To set the stage for the analysis to follow, it is worthwhile to compare the time scale of the pulse to the expected time scale of the electromagnetic response of the cavity. The expected time scale (τ_s) of the cavity is set by the period of oscillation of the lowest mode the cavity can support. A simple estimate for τ_s for a cylindrical cavity is $2.6(\cong 2\pi/2.405)$ times the radial light transit time. In this case τ_s is 6.9 ns. Note that the pulse rise time is about twice as fast as this τ_s and the pulse width is essentially infinite compared to τ_s. It is expected the pulse will excite only the few lowest modes of the cavity. What is unexpected is that the lowest mode has a period of oscillation about four times longer than the above-mentioned simple estimate for τ_s.

For the prescribed axial current source (Fig. 2) at position A in Fig. 1, the code steps Maxwell's equation in time solving for the E_r, E_z, and H_θ fields inside the cavity. The code displays the solution of these fields as either a snap shoot in time over the entire spatial domain of the problem or as a time history at preselected observer points. Examples of the output are displayed in Figs. 3 and 4. Figure 3 is a contour plot of the magnitude of the E_z field at time $t=87.5$ ns. Figure 4 is a time history of H_θ at the observer location indicated as position B in Fig. 1.

A close examination of Fig. 3 indicates that the mode excited by the current pulse is the lowest TM mode of the cavity. It is basically a mode in which the E_z field is constant in z and zero on the outside wall and inner core. The exception is a strong E field gradient across the gap at position A and around the bottom of the spacecraft.

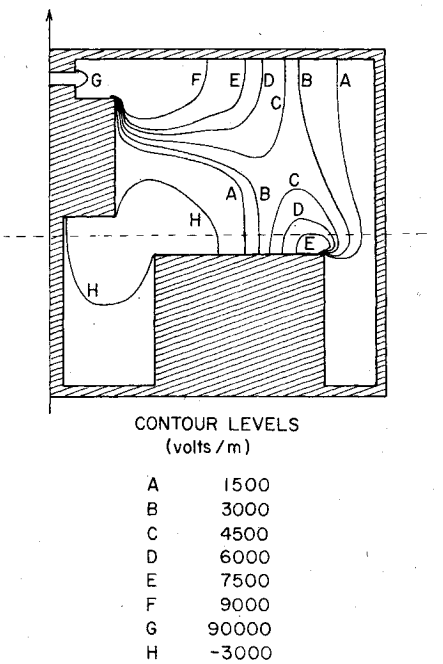

Fig. 3 Contour plot of E_z at $t=87.5$ ns. Contours indicate at TM_{010} mode modified by large electric field gradient across gap (contour G) and internal structure below dashed line. Both modifications significantly distort the mode.

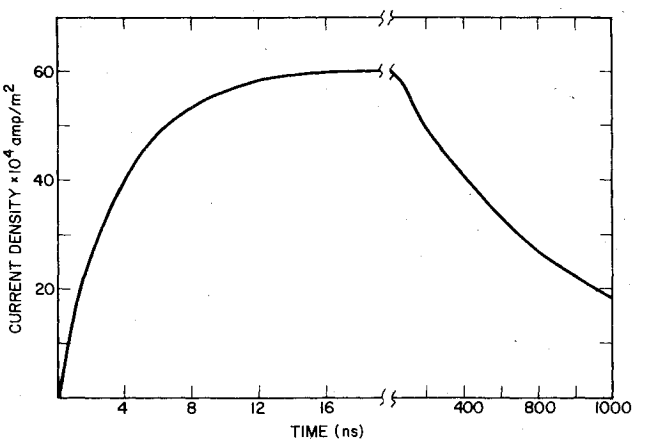

Fig. 2 Time history of the axial current pulse occurring at point A of cavity.

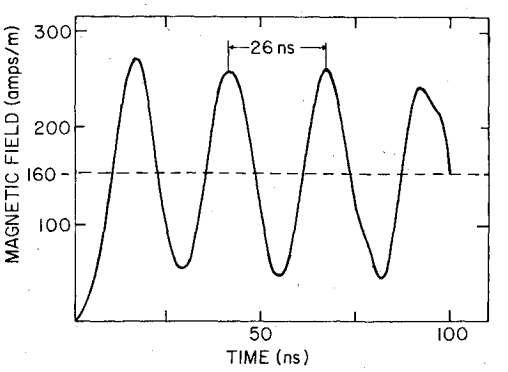

Fig. 4 Magnetic field response calculated at observer location B. Waveform is basically a dc level of 160 A/m and a sin wave of period 26.0 ns which corresponds to a frequency of 38.5 MHz.

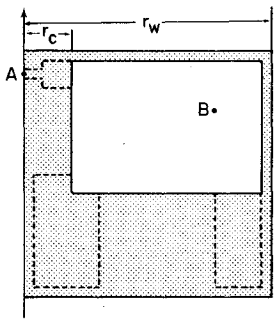

Fig. 5 Simplified version of the cavity in Fig. 1. Shaded area is metallic, dotted lines are the interior boundaries of the original cavity. The TM mode for this cavity with and without the gap at position A are analyzed in text.

Figure 4 indicates a H_θ field that is ringing with the characteristic frequency of the lowest mode, superimposed on a constant field of about 160 A/m. The constant field is readily explained. If we take the line integral H_θ azimuthally around the cylinder and set it equal to the current passing through the enclosed area, we have

$$I=\oint H\mathrm{d}l=H_\theta 2\pi r=784\ \mathrm{A} \tag{2}$$

The current density at point A is 60×10^4 A/m^2. Assuming the current is issued over an area with radius of one-half cell length in the radial direction, we have

$$I=J\times\mathrm{Area}=753\ \mathrm{A}$$

Thus, the dc offset of the H_θ field is just the current through the area enclosed by the field loop, as expected. This can be considered a test of the numerical integration procedures, indicating the code reproduces the electromagnetic response of the cavity to within a few percent.

The second and more perplexing aspect of the time history of the H_θ field is the frequency of its oscillation. From Fig. 4, the period of oscillation is estimated to be 26 ns, which corresponds to a frequency of

$$f=1/26\ \mathrm{ns}=38.5\ \mathrm{MHz}$$

This frequency is four times lower than the expected lowest frequency of the cavity, which can be estimated by using τ_s

$$f=1/\tau_s=145\ \mathrm{MHz}$$

The reason for this discrepancy involves the interplay at the small gap at position A with the cavity resonance mode. This effect is analyzed in detail in the next section by using a simplified version of the cavity structure in Fig. 1.

III. Analysis of Electromagnetic Response of Cavity

The numerical results of the electromagnetic response of the cavity in Fig. 1 shows a fundamental frequency at 38.5 MHz. A simple estimate of the frequency response of the cavity, based on the transit time of light across the cavity, is 145 MHz. In order to explain why this discrepancy occurs, we will analyze in detail the fundamental TM mode of a simplified version of the cavity in Fig. 1. We assume that the actual mode structure corresponds closely to that for the coaxial geometry shown in Fig. 5. The inner radius is taken to be that of the dominant cylinder on axis in the original configuration. Note that the length of the simple system is shorter than that of the original. The length is taken to be the distance from the front face to the large doughnut structure at the back face of the original system. The assumption here is that this structure is sufficiently large so as to be considered simply as a disk. In fact, this is a poor assumption and means that the simplified picture for the back face is not a good approximation to the original geometry, which is too complicated for accurate evaluation of the mode structure by analytical techniques.

We first examine the mode structure for the simple core without a gap. Later, the effect of incorporation of the small gap will be discussed. The frequency analysis of the simplified cavity is a standard mathematical exercise presented in many textbooks.[9] We are interested in the lowest TM mode which is usually referred to as TM_{010}. The E_z field of this mode is constant in z and is zero on the outside wall and inner core. The E_r field is zero. The equations for E_z and H_θ for this mode are

$$(1/r)\,(\partial/\partial r)rH_\theta=i\omega\epsilon E_z \tag{3}$$

$$-i\omega\mu H_\theta=\partial E_z/\partial r \tag{4}$$

where we have assumed $\exp(i\omega t)$ time dependence. The solutions for these equations are Bessel functions of the first and second kind. The general solution for E_z is

$$E_z=AJ_0(\lambda r)+BY_0(\lambda r) \tag{5}$$

where

$$\lambda\equiv\omega/c \tag{6}$$

The condition that E_z be zero on the outer wall specifies the ratio of A and B in Eq. (5), i.e.,

$$E_z=K[\,Y_0(\lambda r_w)J_0(\lambda r)-J_0(\lambda r_w)\,Y_0(\lambda r)\,] \tag{7}$$

where K is an arbitrary constant and r_w the outer wall radius. The remaining boundary condition, that of E_z being zero on the inner core, determines the eigenvalue λ.

In order to represent the inner boundary condition graphically, we will first calculate the core impedance of a particular TM_{0n0} cavity mode. The core impedance is simply defined as the ratio of the voltage across the length of the core and the current flowing along the core. In this case,

$$Z_c=V/I=\int_0^L E_z\mathrm{d}_z\Big/\int_0^{2\pi}H_\theta r_c\mathrm{d}_\theta=LE_z/2\pi r_cH_\theta$$

where L is the length of the cylinder and r_c is the core radius.

Using Eq. (4) and Eq. (7)

$$Z_c(r\mid r_w,\lambda)$$

$$=\frac{-iL}{2\pi r_c}\sqrt{\frac{\mu}{\epsilon}}\left[\frac{Y_0(\lambda r_w)J_0(\lambda r)-J_0(\lambda r_w)\,Y_0(\lambda r)}{Y_0(\lambda r_w)J_1(\lambda r)-J_0(\lambda r_w)\,Y_1(\lambda r)}\right](\mathrm{ohms}) \tag{8}$$

From Eq. (8), we see that the condition $E_z=0$ on the inner core ($r=r_c$) can be interpreted as the core impedance of the cavity mode being zero (short circuit). A graph of $Z_c(r_c\mid r_w,\lambda)$ vs $\lambda c/2\pi$ is given in Fig. 6 (solid lines). Z_c has a countable infinity of discontinuities. Between each discontinuity is a branch of the curve that corresponds to a particular TM_{0n0} mode. The point where a particular branch crosses zero gives the frequency of oscillation for the particular TM_{0n0} mode for the cavity pictured in Fig. 5. Note that the frequency for the lowest branch is zero. The first nonzero frequency is located on the second branch and corresponds to the TM_{010} mode. For this case, the frequency is

$$\lambda c/2\pi=f=182\ \mathrm{MHz}$$

The addition of the gap changes the mode structure found for the simple core model. Whereas the impedance of the simple core is zero by virtue of $E_z=0$ at the core surface, a

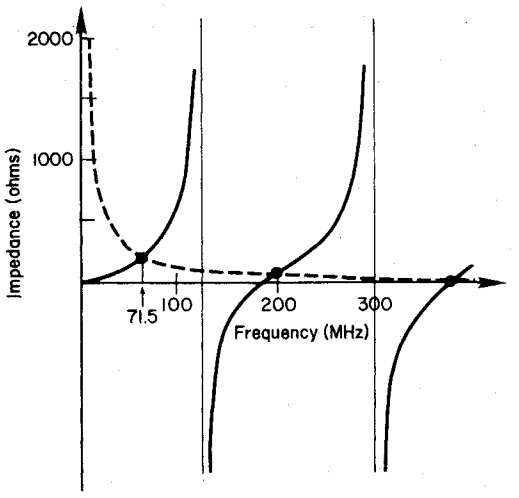

Fig. 6 Core impedance (solid lines) and gap impedance (dashed line) vs frequency for simplified cavity. Core impedance is $Z_c(r_c \mid r_w, \lambda)$ as defined in Eq. (8) where $r_c = 20$ cm, $r_w = 100$ cm, and $\lambda = 2\pi f/c$. Gap impedance Z_{gap} is for capacitor of 12.3 $\mu\mu f$. Dots are solutions to $Z_c = Z_{gap}$. First solution is at 71.5 MHz.

small gap will cause a nonzero E_z field to develop within a short radial distance from the core surface. The core impedance defined at this position will no longer be zero.

We now argue that the value of the core impedance must match the capacitive impedance of the gap. The core current $(2\pi r_c H_\theta)$ is forced to flow through the gap capacitance creating a voltage which is easily computed by knowing the capacitive gap impedance. This voltage appears as a strong E_z field across the gap which diffuses out into the cavity. Away from the direct vicinity of the gap and the core boundary, the cavity mode behaves as if it sees the gap voltage across the whole length of the core. Therefore, at a small distance away from the core boundary, the axial field is related to the gap field E_g by the relation

$$E_z = dE_g/L$$

where d is the effective gap spacing. This expression is the only one that yields a z field constant in the z direction and that also guarantees zero potentials close to each end of the cavity. This procedure is just equivalent to the requirement of impedance matching. The approximation is good as long as the scale length of the wave is large compared to the radius of the core,[10] which is the case for the TM_{010} modes.

We choose a gap at the same position and with the same dimensions as for the original cavity (Fig. 1). The impedance of the gap in this case is the result of two capacitances in parallel, the center disk capacitor being of radius 8 cm and gap length 4 cm, and the outer annular capacitor with a radius extending from 8 to 20 cm and a gap width of 12 cm (see Fig. 1).

Calculating the gap impedance, we then have

$$Z_{gap} = 1/i\omega C_{gap}$$

$$C_{gap} = \frac{\epsilon_0 \pi (0.08)^2}{0.04} + \frac{\epsilon_0 \pi (0.2^2 - 0.08^2)}{0.12} = 12.3 \mu\mu f$$

Z_{gap} vs $f = \lambda c/2\pi$ is also plotted on Fig. 6 (dashed line). If indeed the cavity mode core impedance has to match the gap impedance to satisfy the inner boundary condition, the intersection of Z_{gap} and Z_c in Fig. 6 represents mode frequencies of the cavity in Fig. 5 with the insertion of the gap in Fig. 1. Now the lowest frequency has a very different character. It is

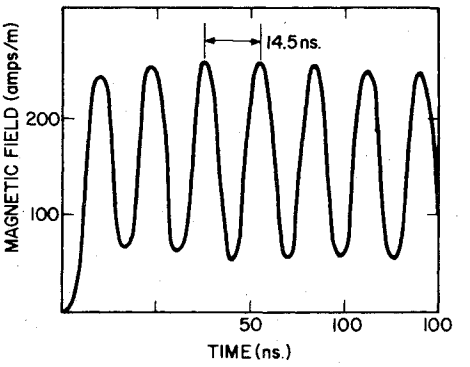

Fig. 7 Magnetic field response calculated at position B for simplified cavity with gap and driving current of original cavity. Period of oscillation is 14.5 ns which corresponds to a frequency of 68.9 MHz. This compares favorably with analytic prediction of 71.5 MHz based on equating cavity mode core impedance and gap impedance.

located on the lowest branch of the core impedance curve, the branch that has the zero solution for the short circuit inner boundary condition. Depending on the value of the gap capacitance, the lowest frequency mode can range from zero to the lower cutoff of the TM_{010} mode. The frequency of oscillation has very little to do with the length scale of the cavity—as in our initial estimation of the lowest oscillation period of the cavity. Our estimate of the lowest oscillation period of the cavity relates to the TM_{010} mode that corresponds to the second branch of the wave impedance.

To verify this argument numerically, we computed the electromagnetic response of the simplified cavity including the gap plus the current driver. The H_θ response at location B of the simplified structure is shown in Fig. 7. From this graph, we read the period of oscillation as 14.5 ns. This corresponds to a frequency of

$$f = 1/14.5 \text{ ns} = 68.9 \text{ MHz}$$

This agrees well with the value of 71.5 MHz for the lowest frequency at which $Z_{gap} = Z_c$, read from Fig. 6.

The original cavity shown in Fig. 1 had a frequency response at 38.5 MHz. The difference between this value and the frequency response of the simplified cavity, which was 68.9 MHz, can be attributed to an increased length in the z direction and by the inductive loading of the added internal structure. Since now the added internal structure has the same length scale of the electromagnetic wave, it is not worthwhile to treat this inductive loading as we did the capacitive impedance of the gap. In fact, the only reliable way to analyze the effect of the added internal structure apart from conducting an experiment is to run a numerical code, as we have demonstrated.

IV. Conclusions

The effect of small gaps on the electromagnetic properties of an internal cavity can be considerable. For strategically placed gaps, the cavity can resonate at a frequency two or three times lower than what would be estimated from length and time scale arguments for the cavity. For the case presented in this paper, "strategically placed" meant the gap cut the main wall current driven by the TM_{010} mode. This caused the wall currents from the faces of the cylinder to feed the capacitor plates created by the gap. In the vacuum around the gap, the gap's capacitive impedance manifested itself as the core impedance of the electromagnetic oscillations. This led to an inner boundary condition that permitted a mode of oscillation that was not accessible without the gap. On a practical level, this exercise demonstrates the ability of a straightforward numerical code in conjunction with simple circuit theory to analyze the effects complex structures have on electromagnetic oscillations.

References

[1] Deforest, S. and Goldstein, R., "A Study of Electrostatic Charging of ATS-S Satellite Dump Ion Thruster Operation," Final Technical Report JPL 73-199, Dec. 1973.

[2] Nanevitz, J. E., Adamo, R. C., and Beers, B. L., "Characterization of Electromagnetic Signals Generated by Electrical Breakdown of Spacecraft Insulating Materials," Air Force Geophysics Laboratory Rept. AFGL-TR-79-0082, 1979.

[3] Rosen, A., "Large Discharge and Arcs on Spacecraft," *Astronautics & Aeronautics,* Vol. 13, June 1975, pp. 36-44.

[4] Treadway, M. J. et al, "Experimental Verification of ECEMP Spacecraft Discharge Coupling Model," *IEEE Transactions on Nuclear Science,* Vol. NS-127, Dec. 1980, pp. 1776-1779.

[5] Stevens, J. N., *Spacecraft Charging Technology Conference,* sponsored by NASA/Air Force System Command, Proceedings to be published as AFGL Technical Report.

[6] Rosen, A., Sanders, N. L., Sellen, J. M. Jr., and Inouye, G. T., "Effects of Arcing Due to Spacecraft Charging of Spacecraft Survival," TRW Rept. 33631-6006-RU-00, Nov. 1978.

[7] Goplin, B., Clark, R., and Fishbone, B., "MAD2—A Computer Code for SGEMP Calculations in Two Dimensions," SAI Rept. SAI-76-505-AQ, 1976.

[8] O'Donnell, E. E., Private communications, Jan. 1979.

[9] Jackson, J. D., "Wave Guides and Resonant Cavities," *Classical Electrodynamics,* John Wiley & Sons, New York, 1962, pp. 235-267.

[10] Ramo, R. and Whinnery, J. R., "Resonant Cavities," *Fields and Waves in Communication Electronics,* John Wiley & Sons, New York, 1965, pp. 558-561.